Spacecraft Attitude Control Using Magnetic and Mechanical Actuation

Emanuele L. de Angelis[1] and Fabrizio Giulietti[2]
Università di Bologna, 47121 Forlì, Italy

Anton H.J. de Ruiter[3]
Ryerson University, M5B 2K3 Toronto, Canada

Giulio Avanzini[4]
Università del Salento, 73100 Lecce, Italy

The aim of this paper is the analysis of simultaneous attitude control and momentum-wheel management of a spacecraft by means of magnetic actuators only. A proof of almost global asymptotic stability is derived for control laws that drive a rigid satellite toward attitude stabilization in the orbit frame, when the momentum-wheel is aligned with one of the principal axes of inertia. Performance of the proposed control laws is demonstrated by numerical simulations under actuator saturation. Robustness to external disturbances and model uncertainties is also evaluated.

Nomenclature

$\boldsymbol{b}$	Geomagnetic field vector expressed in $\mathbb{F}_B$, T
C_D	Spacecraft drag coefficient
$\hat{\boldsymbol{e}}_1, \hat{\boldsymbol{e}}_2, \hat{\boldsymbol{e}}_3$	Spacecraft principal axes of inertia
$\mathbb{F}_B$	Body-fixed frame

[1] Research Fellow, Department of Industrial Engineering (DIN), Via Fontanelle 40; emanuele.deangelis4@unibo.it (Corresponding Author).
[2] Associate Professor, Department of Industrial Engineering (DIN), Via Fontanelle 40, AIAA Senior Member; fabrizio.giulietti@unibo.it.
[3] Associate Professor, Department of Aerospace Engineering, AIAA Senior Member; aderuiter@ryerson.ca.
[4] Professor, Department of Engineering for Innovation (DII), Complesso Ecotekne (Corpo O), Via per Monteroni, AIAA Senior Member; giulio.avanzini@unisalento.it.

$\mathbb{F}_I$	Inertial frame
$\mathbb{F}_O$	Local-vertical/local-horizontal orbit frame
$\boldsymbol{h}$	$= (0, h, 0)^T$ Angular momentum of the wheel relative to $\mathbb{F}_B$, N m s
i	Orbit inclination, deg
$\boldsymbol{I}_3$	3×3 identity matrix
g	Torque on the momentum-wheel, N m
$\boldsymbol{J}$	Spacecraft inertia matrix, kg m^2
J_w	Moment of inertia of the momentum-wheel, kg m^2
$k, k_\varepsilon, k_\zeta, \lambda$	Control gains, s^{-1}, s^{-1}, s^{-1}, rad^{-1} s^{-1}
l_1, l_2, l_3	Spacecraft dimensions, m
$\boldsymbol{M}$	$= (M_1, M_2, M_3)^T$ External torque acting on the spacecraft, N m
$\boldsymbol{m}$	$= (m_1, m_2, m_3)^T$ Magnetic dipole moment vector, A m^2
n	Orbit rate, rad s^{-1}
$\hat{\boldsymbol{o}}_1, \hat{\boldsymbol{o}}_2, \hat{\boldsymbol{o}}_3$	Orbital axes
r_c	Orbit radius, km
T	Orbit period, s
$\boldsymbol{T}_{BI}$	Coordinate transformation matrix between $\mathbb{F}_I$ and $\mathbb{F}_B$
$\boldsymbol{T}_{BO}$	Coordinate transformation matrix between $\mathbb{F}_O$ and $\mathbb{F}_B$
$\boldsymbol{V}$	$= (V, 0, 0)^T$ Translational velocity along the orbit, m s^{-1}
$\boldsymbol{0}_{m \times n}$	$m \times n$ zero matrix

Greek symbols

$\boldsymbol{\varepsilon}$	$= (\varepsilon_1, \varepsilon_2, \varepsilon_3)^T$ Body angular momentum error, N m s
Ω	Wheel spin rate relative to the spacecraft, rad s^{-1}
$\boldsymbol{\omega}$	$= (\omega_1, \omega_2, \omega_3)^T$ Spacecraft angular velocity vector relative to $\mathbb{F}_I$, rad s^{-1}
$\boldsymbol{\omega}^r$	$= (\omega_1^r, \omega_2^r, \omega_3^r)^T$ Spacecraft angular velocity vector relative to $\mathbb{F}_O$, rad s^{-1}
ψ, ϕ, θ	3-1-2 Euler angle sequence, rad
ρ	Air density, kg m^{-3}
$\hat{\boldsymbol{\sigma}}$	$= \boldsymbol{T}_{BO}\,(0, 1, 0)^T$ Unit vector along the orbit normal

$\boldsymbol{\zeta} = (\zeta_1, \zeta_2, \zeta_3)^T$ Inertial angular momentum error, N m s

Subscripts

$_0$ Initial condition at time t_0

$_d$ Desired value

$_I$ Vector components in the inertial frame $\mathbb{F}_I$

$_{max}$ Maximum

$_{min}$ Minimum

$_O$ Vector components in the orbit frame $\mathbb{F}_O$

I. Introduction

In this paper, the control of a spacecraft using both magnetic and mechanical actuation is considered. A proof of almost global asymptotic stability is derived for control laws that drive a rigid satellite toward attitude stabilization in the orbit frame.

Modern small-scale spacecraft are often provided with magnetorquers (MTs) and some kind of mechanical actuators (e.g., reaction and/or momentum-wheels). The former are generally used for detumbling purpose after the release of the spacecraft from the launch vehicle [1] and for momentum dumping of reaction-wheels during desaturation maneuvers [2]. The latter are used for fine pointing control and attitude stabilization in the presence of external disturbance torques. This is the case of the European Student Earth Orbiter (ESEO), a micro-satellite mission to Low Earth Orbit (LEO) that is being developed, integrated, and tested by European university students as an ESA Education Office project [3]. In this platform, three-axis pointing with respect to the orbit frame is required for Earth observation and the attitude control system is equipped with a set of magnetorquers and one pitch momentum-wheel (MW) performing the control logic described in this paper.

As a matter of fact, magnetic and mechanical devices are seldom used simultaneously. The combined use of the two actuation systems would actually lead to power saving and less stringent requirements on the wheel control torques. In Refs. [4, 5], inertial pointing of a spacecraft using magnetic actuation only was considered. Owing to the time-varying nature of the system, bounds on the choice of the proportional-derivative gains resulted, which in turn lead to closed-loop performance

limitations. Stability (and proof thereof) was based on averaging theory, which physically translates to the system possessing certain dynamic properties on average. Attitude control of spacecraft using two actuation systems was considered in [6], where the magnetic command law proposed in [5] was used in concert with the control action of a set of reaction-wheels, thus mitigating the above limitations. In [7] attitude control a hybrid controller based on MTs and thrusters was proposed, with a linear time-periodic approach and the analysis of actuator saturation. A geometric scheme was proposed in [8], where the desired control vector was decomposed in terms of orthogonal and parallel components with respect to the direction of the local geomagnetic field vector. The orthogonal component was actuated by MTs, whereas the parallel component was generated by a set of one, two, or three wheels.

In a recent paper [9], three of the authors of the present work proposed a control law that leads a spacecraft to acquire a desired pure spin condition around one of the principal axes of inertia by means of magnetic actuators only, while aiming the spin axis toward a prescribed direction in the inertial space. A similar approach is used in this framework, where the error dynamics equation is first derived for two error signals, namely the angular momentum error in the body frame and the angular momentum error with respect to the desired direction of the wheel spin axis in the inertial frame. The error dynamics is then recast in the classical form of a nominal system perturbed by a vanishing perturbation term. After proving global exponential stability for the nominal system controlled by MTs, the result discussed in [9] is here extended to the perturbed one. As a further contribution, full three-axis attitude stabilization is obtained (rather than simple spin-axis pointing) by means of a proper choice of the wheel control law governing the pitch angle dynamics. A similar approach was described in [10], where attitude stabilization was performed by means of a set of three MWs and three MTs, while the angular momenta of the MWs were driven to given reference values. In that case, the mechanical system provided attitude stabilization with respect to the inertial frame, letting the rank-deficient magnetic torque be only used for momentum dumping of the wheel set. Magnetic controllability was discussed and assumptions were made on the magnetic field vector, supposed to be capable of persistently spanning all of the 3-D space over one orbit. Finally, the proposed control scheme was proven to lead to a real cascade system where attitude

dynamics is completely independent of momentum dumping.

The derivation by means of nonlinear control techniques of a hybrid control system relying on a combination of a single mechanical actuator with magnetic torquers thus represents the major contribution of the present work, where complete attitude stabilization over an inclined orbit is obtained in those cases when angular rate and attitude measurements are available. In what follows, system dynamics and attitude parametrization are described in Section II. The proposed control laws and the closed-loop stability analysis are discussed in Section III, where the cascade structure of the overall system is pointed out. Numerical simulations in Section IV support the findings in a realistic scenario, featuring the most relevant disturbance torques in LEO. Concluding remarks end the paper.

II. System Dynamics

A. Angular Momentum Balance

A sketch of the spacecraft, featuring one MW and three mutually orthogonal MTs is represented in Fig. 1. The spacecraft is assumed to be rigid. The evolution of angular velocity components is derived from the angular momentum balance equation projected onto a frame of body axes, $\mathbb{F}_B = \{P; \hat{\boldsymbol{e}}_1, \hat{\boldsymbol{e}}_2, \hat{\boldsymbol{e}}_3\}$, centered in the spacecraft center of mass P:

$$\boldsymbol{J}\dot{\boldsymbol{\omega}} + \dot{\boldsymbol{h}} + \boldsymbol{\omega} \times (\boldsymbol{J}\boldsymbol{\omega} + \boldsymbol{h}) = \boldsymbol{M}^{(c)} + \boldsymbol{M}^{(d)} \tag{1}$$

where $\boldsymbol{\omega} = (\omega_1, \omega_2, \omega_3)^T$ is the absolute angular velocity vector of the spacecraft, $\boldsymbol{J}$ is the spacecraft inertia matrix, and $\boldsymbol{h}$ is the angular momentum of the wheel relative to $\mathbb{F}_B$. In the proof of closed-loop stability of the control law, it will be initially assumed that $\boldsymbol{J} \equiv \boldsymbol{J}^* = \mathrm{diag}(J_1, J_2, J_3)$, that is, $\hat{\boldsymbol{e}}_1$, $\hat{\boldsymbol{e}}_2$, and $\hat{\boldsymbol{e}}_3$ are principal axes of inertia, and $J_2 \neq J_1, J_3$. The presence of off-diagonal terms in $\boldsymbol{J}$ and uncertainties on the elements of $\boldsymbol{J}$ will be dealt within the Results section, in order to assess control law robustness. In the most general case, the MW relative angular momentum is $\boldsymbol{h} = J_w \Omega \, \hat{\boldsymbol{a}}$, where J_w is the moment of inertia of the wheel about its spin axis $\hat{\boldsymbol{a}}$, and Ω is the wheel spin rate with respect to the spacecraft. Letting $h = J_w \Omega$, one obtains

$$\dot{h} = g - J_w \, \dot{\boldsymbol{\omega}}^T \hat{\boldsymbol{a}} \tag{2}$$

where g is the torque applied to the wheel about its spin axis by its electric motor. Assuming that $\hat{\boldsymbol{a}} \equiv \hat{\boldsymbol{e}}_2$ (that is, the wheel spins around an axis parallel to the spacecraft pitch axis) leads to $\boldsymbol{h} = (0, h, 0)^T$, and Eq. (2) reduces to the scalar equation:

$$\dot{h} = g - J_w \dot{\omega}_2 \tag{3}$$

In the ideal case when the wheel assembly is not affected by friction, g represents the control input. Alternatively, it is possible to take $\dot{h}$ directly to be the control input for the pitch control law design. This is often done in practice, removing any argument over whether or not friction needs to be accounted for.

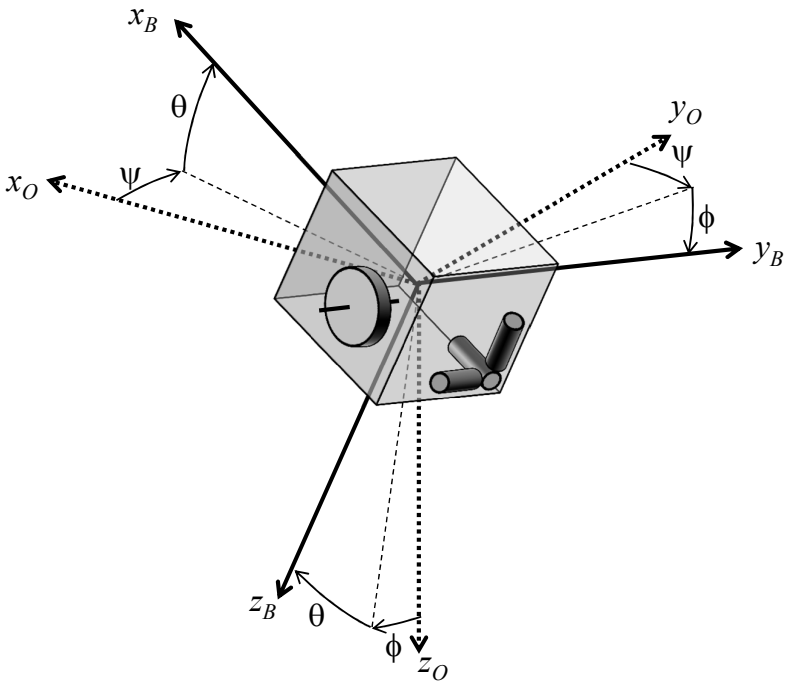

Figure 1 Sketch of the spacecraft (with definition of the attitude variables).

No external disturbance $\boldsymbol{M}^{(d)}$ is considered in the stability analysis, so that the external torque acting on the spacecraft coincides with the magnetic control torque, namely $\boldsymbol{M}^{(c)} = \boldsymbol{m} \times \boldsymbol{b}$, where $\boldsymbol{m}$ is the magnetic dipole moment vector generated by the MTs and $\boldsymbol{b} = \boldsymbol{T}_{BO}\, \boldsymbol{b}_O$ is the local geomagnetic field vector expressed in terms of body-frame components. A circular LEO of radius r_c, period T, and orbit rate $n = 2\pi/T$ is considered. The components $\boldsymbol{b}_O$ of the geomagnetic field are provided in the local-vertical/local-horizontal orbit frame, $\mathbb{F}_O$, by means of the International Geomagnetic Reference Field (IGRF) model [11, 12], provided the z_O-axis lies along the local vertical

pointing upwards, the y_O-axis is normal to the orbit plane, in the direction of the orbital angular speed $\boldsymbol{\omega}^{orb}$, and the transverse axis x_O completes a right-handed triad. For a circular orbit, x_O is parallel to the direction of the orbital velocity.

B. Attitude Kinematics

The attitude of the spacecraft with respect to $\mathbb{F}_O$ is described by means of an unconventional 3-1-2 Euler angle sequence, where the "yaw" angle ψ around the local vertical z_O is given by the angular distance between the y_O-axis and the projection of y_B on the orbit plane, whereas the "roll" angle ϕ is represented by the elevation of y_B with respect to the orbit plane. The sequence of elementary rotations is completed by a "pitch" rotation θ around the unit vector $\hat{\boldsymbol{e}}_2$, parallel to y_B, as represented in Fig. 1. The coordinate transformation matrix between $\mathbb{F}_O$ and $\mathbb{F}_B$, parametrized by means of the 3-1-2 Euler sequence is:

$$\boldsymbol{T}_{BO} = \begin{pmatrix} \mathrm{c}\psi\mathrm{c}\theta - \mathrm{s}\phi\mathrm{s}\psi\mathrm{s}\theta & \mathrm{c}\theta\mathrm{s}\psi + \mathrm{c}\psi\mathrm{s}\phi\mathrm{s}\theta & -\mathrm{c}\phi\mathrm{s}\theta \\ -\mathrm{c}\phi\mathrm{s}\psi & \mathrm{c}\phi\mathrm{c}\psi & \mathrm{s}\phi \\ \mathrm{c}\psi\mathrm{s}\theta + \mathrm{c}\theta\mathrm{s}\phi\mathrm{s}\psi & \mathrm{s}\psi\mathrm{s}\theta - \mathrm{c}\psi\mathrm{c}\theta\mathrm{s}\phi & \mathrm{c}\phi\mathrm{c}\theta \end{pmatrix} \tag{4}$$

where $\mathrm{c}(\cdot) = \cos(\cdot)$ and $\mathrm{s}(\cdot) = \sin(\cdot)$. Euler angles evolve as a function of the angular speed of the spacecraft relative to $\mathbb{F}_O$, given by $\boldsymbol{\omega}^r = \boldsymbol{\omega} - \boldsymbol{T}_{BO}\,\boldsymbol{\omega}_O^{orb}$, where $\boldsymbol{\omega}_O^{orb} = (0, n, 0)^T$ is the angular speed of $\mathbb{F}_O$ with respect to an inertial frame $\mathbb{F}_I$, with components expressed in $\mathbb{F}_O$ [13]. The kinematics of yaw, roll, and pitch angles can be written as a function of the angular speed of the spacecraft relative to $\mathbb{F}_O$, namely

$$\omega_1^r = \dot{\phi}\cos\theta - \dot{\psi}\cos\phi\sin\theta \tag{5}$$

$$\omega_2^r = \dot{\theta} + \dot{\psi}\sin\phi \tag{6}$$

$$\omega_3^r = \dot{\phi}\sin\theta + \dot{\psi}\cos\phi\cos\theta \tag{7}$$

or in terms of the absolute angular velocity vector of the spacecraft, $\boldsymbol{\omega} = \boldsymbol{\omega}^r + n\boldsymbol{T}_{BO}\hat{\boldsymbol{o}}_2$:

$$\omega_1 = \dot{\phi}\cos\theta - \dot{\psi}\cos\phi\sin\theta + n\,(\cos\theta\sin\psi + \sin\phi\sin\theta\cos\psi) \tag{8}$$

$$\omega_2 = \dot{\theta} + \dot{\psi}\sin\phi + n\,\cos\phi\cos\psi \tag{9}$$

$$\omega_3 = \dot{\phi}\sin\theta + \dot{\psi}\cos\phi\cos\theta + n\,(\sin\theta\sin\psi - \sin\phi\cos\theta\cos\psi) \tag{10}$$

In the latter case, the kinematics of Euler angles in Eqs. (8), (9), and (10) is conveniently rearranged as follows:

$$\dot{\psi} = (-\omega_1 \sin\theta + \omega_3 \cos\theta + n \sin\phi\cos\psi) / \cos\phi \tag{11}$$

$$\dot{\phi} = \omega_1 \cos\theta + \omega_3 \sin\theta - n \sin\psi \tag{12}$$

$$\dot{\theta} = \omega_2 + (\omega_1 \sin\phi\sin\theta - \omega_3 \sin\phi\cos\theta - n\cos\psi) / \cos\phi \tag{13}$$

The use of Euler angles requires some attention, since singular configurations always occur when attitude is represented by means of a sequence of three elementary rotations. In the present case, when the second rotation ϕ is equal to ± 90 deg, the pitch axis coincides with the local vertical, and the first and third rotations are performed around the same axis. On the other hand, this situation is unlikely to be encountered in practice, for the rotation sequence here adopted. In fact, after a spacecraft is injected into its orbit, an initial detumbling maneuver is performed in order to dump the angular momentum accumulated during payload ejection. During this phase, when the attitude information is not yet available because of the high rotation rates, the spacecraft is typically driven toward a pure spin condition by means of a B-dot like control law [14], such that the spin axis gets sufficiently close to the normal to the orbit plane and small values of the angles ψ and ϕ are expected [15]. This means that $\phi = \pm 90$ deg is an unlikely situation and the applicability of the control law described in this paper is not at stake.

Conversely, when a residual pitch rate is expected, both the classical yaw-pitch-roll (3-2-1) and precession-nutation-spin (3-1-3) sequences will approach singular configurations during the satellite motion, thus harming practical applicability of the control law and possibly hindering the search for closed-loop stability proofs. This motivates the choice of this unusual Euler angle sequence in the description of spacecraft attitude kinematics.

C. External Disturbances

In order to assess robustness of the control laws proposed in the next Section, the three most relevant sources of external disturbance torque in LEO are included in the model used for the simulations discussed in the Results section, namely gravity gradient, aerodynamic, and residual magnetic torques [11].

For a circular orbit, gravity gradient torque is given by

$$\boldsymbol{M}^{(gg)} = 3n^2 \left[\hat{\boldsymbol{o}}_3 \times (\boldsymbol{J}\hat{\boldsymbol{o}}_3)\right] \tag{14}$$

where $\hat{\boldsymbol{o}}_3$ is the unit vector parallel to the local vertical.

The interaction of the upper atmosphere molecules with the external surface of the satellite introduces an aerodynamic torque. Following the derivation discussed in some detail in [16] and summarized in [11], it is possible to assume that the incident air particles lose their entire energy on collision. The force $\mathrm{d}\boldsymbol{f}_a$ on a surface element $\mathrm{d}A$, with outward normal $\hat{\boldsymbol{n}}$, is thus given by

$$\mathrm{d}\boldsymbol{f}_a = -\frac{1}{2}\rho V^2 C_D \left(\hat{\boldsymbol{n}} \cdot \hat{\boldsymbol{v}}\right) \hat{\boldsymbol{v}} \mathrm{d}A \tag{15}$$

where $\hat{\boldsymbol{v}} = \boldsymbol{V}/||\boldsymbol{V}||$ is the unit vector in the direction of the translational velocity, $\boldsymbol{V}$, of the surface element relative to the incident stream, ρ is the density of the rarefied air at the considered orbit altitude, and C_D is a drag coefficient. The aerodynamic torque $\boldsymbol{M}^{(a)}$ acting on the spacecraft due to the force $\mathrm{d}\boldsymbol{f}_a$ is

$$\boldsymbol{M}^{(a)} = \int \boldsymbol{r}_s \times \mathrm{d}\boldsymbol{f}_a \tag{16}$$

where $\boldsymbol{r}_s$ is the vector from the spacecraft center of mass to the surface element $\mathrm{d}A$ and the integral is evaluated over the spacecraft surface for which $\hat{\boldsymbol{n}} \cdot \hat{\boldsymbol{v}} > 0$. When the surface area can be decomposed into simple flat geometric shapes (as in the case of the six faces of a parallelepiped satellite), the overall torque can be calculated as the vector sum of the individual torques given by the cross product of the vector joining the spacecraft center of mass to the center of pressure of each geometric shape times the force acting on the component.

The residual magnetic torque $\boldsymbol{M}^{(rm)}$ is produced by the overall dipole moment $\boldsymbol{m}_{rm}$ generated by on-board electrical systems and circuits. When magnetic coils are active, the residual dipole moment is relatively negligible, but when they are switched off, it produces a significant contribution to the disturbance torque:

$$\boldsymbol{M}^{(rm)} = \boldsymbol{m}_{rm} \times \boldsymbol{b} \tag{17}$$

III. Attitude Stabilization

In what follows, simultaneous attitude control and momentum-wheel management of a spacecraft using magnetic actuation is examined. Control laws are proposed and asymptotic convergence is proven, when the variation of Earth magnetic field in the orbit frame is taken into account.

A. Control Laws

Let $\hat{\boldsymbol{\sigma}} = \boldsymbol{T}_{BO}\,(0,1,0)^T$ be the unit vector parallel to the direction of the y_O-axis, fixed in both the orbit and inertial frames, and Ω_d be the desired spin rate of the wheel with respect to the spacecraft. Two desired angular momentum vectors, $\boldsymbol{h}_d$ and $\boldsymbol{H}_d$, are defined in the body-fixed and in the inertial frames, respectively. Letting $h_d = J_w\,\Omega_d + J_2\,n$, the first one is defined as $\boldsymbol{h}_d = (0, h_d, 0)^T$, which is used to enforce that the angular momentum vector becomes parallel to the pitch axis. The second one is given by $\boldsymbol{H}_d = h_d \hat{\boldsymbol{\sigma}}$, which requires that the angular momentum points in the desired inertially-fixed direction parallel to the orbit normal. Two different angular momentum error variables are thus introduced, namely

$$\boldsymbol{\zeta} = \boldsymbol{H}_d - \boldsymbol{h} - \boldsymbol{J}\,\boldsymbol{\omega} \tag{18}$$

and

$$\boldsymbol{\varepsilon} = \boldsymbol{h}_d - \boldsymbol{h} - \boldsymbol{J}\,\boldsymbol{\omega} \tag{19}$$

where all the vector quantities, including $\boldsymbol{H}_d$, are expressed in terms of body frame components [9]. Finally, let $\hat{\boldsymbol{b}} = \boldsymbol{b}/||\boldsymbol{b}||$ be the unit vector parallel to the local geomagnetic field.

The scope of this section is to prove that, on an inclined LEO, the combined use of a simple linear control law for the magnetorquers and a PD-like command law for a mechanical actuator represented by a momentum-bias wheel parallel to the pitch axis, stabilize spacecraft attitude in the orbit frame, while driving the wheel spin rate to the desired value, Ω_d. The control laws are given by

$$\boldsymbol{M}^{(c)} = \left(\boldsymbol{I}_3 - \hat{\boldsymbol{b}}\,\hat{\boldsymbol{b}}^T\right)\,(k_\zeta\,\boldsymbol{\zeta} + k_\varepsilon\,\boldsymbol{\varepsilon}) \tag{20}$$

with $k_\zeta > 0$ and $k_\varepsilon > 0$, for the MT, and

$$\dot{h} = J_2\,\left[\lambda\,\dot{\theta} + k\,\left(\lambda\,\theta - n + \omega_2\right)\right] \tag{21}$$

with $\lambda > 0$ and $k > 0$, for the MW. When represented in terms of body-frame components, the dynamics of the desired angular momentum vector, $\boldsymbol{H}_d$, is given by

$$\dot{\boldsymbol{H}}_d = -\boldsymbol{\omega} \times \boldsymbol{H}_d \tag{22}$$

From the definition of the error in Eq. (18) and taking into account the control law in Eq. (20), one has

$$\dot{\boldsymbol{\zeta}} = -\left(\boldsymbol{I}_3 - \hat{\boldsymbol{b}}\,\hat{\boldsymbol{b}}^T\right)\,(k_\zeta\,\boldsymbol{\zeta} + k_\varepsilon\,\boldsymbol{\varepsilon}) - \boldsymbol{\omega} \times \boldsymbol{\zeta} \tag{23}$$

At the same time, $\boldsymbol{h}_d$ is a constant vector in body axes. Thus the body frame angular momentum error dynamics achieves the form:

$$\dot{\boldsymbol{\varepsilon}} = -\left(\boldsymbol{I}_3 - \hat{\boldsymbol{b}}\,\hat{\boldsymbol{b}}^T\right)\,(k_\zeta\,\boldsymbol{\zeta} + k_\varepsilon\,\boldsymbol{\varepsilon}) + \boldsymbol{\omega} \times (\boldsymbol{h}_d - \boldsymbol{\varepsilon}) \tag{24}$$

B. Momentum Management

Let the inverse of the inertia matrix, $\boldsymbol{J}^{-1}$, be considered as the sum of two contributions, the first being related to an axisymmetric configuration, $\boldsymbol{J}_a^{-1} = \mathrm{diag}(1/\bar{J}, 1/J^\star, 1/\bar{J})$, where $\bar{J}$, $J^\star \in \mathbb{R}^+$ and $\bar{J} \neq J^\star$, the second being a perturbation term such that $\boldsymbol{J}^{-1} = \boldsymbol{J}_a^{-1} + \boldsymbol{\Delta}$, provided $\boldsymbol{\Delta} = \mathrm{diag}(\delta_1, \delta_2, \delta_3)$, $\delta_1\,, \delta_2\,, \delta_3 \in \mathbb{R}$. Without loss of generality, one can assign $J^\star = J_2$ and $\bar{J} = (J_1 + J_3)/2$. In this case, one has $\delta_2 = 0$, $\delta_1 = \sigma/J_1$ and $\delta_3 = -\sigma/J_3$, where $\sigma = (J_3 - J_1)/(J_1 + J_3)$.

Taking into account the considerations above and conveniently rewriting the error dynamics in Eqs. (23) and (24) in terms of inertial components, it follows that

$$\dot{\boldsymbol{Z}} = -\left[\boldsymbol{T}_{BI}^T\left(\boldsymbol{I}_3 - \hat{\boldsymbol{b}}\,\hat{\boldsymbol{b}}^T\right)\boldsymbol{T}_{BI}\right](k_\zeta\,\boldsymbol{Z} + k_\varepsilon\,\boldsymbol{E}) \tag{25}$$

$$\dot{\boldsymbol{E}} = -\left[\boldsymbol{T}_{BI}^T\left(\boldsymbol{I}_3 - \hat{\boldsymbol{b}}\,\hat{\boldsymbol{b}}^T\right)\boldsymbol{T}_{BI}\right](k_\zeta\,\boldsymbol{Z} + k_\varepsilon\,\boldsymbol{E}) - \boldsymbol{T}_{BI}^T\left\{\left[\left(\boldsymbol{J}_a^{-1} + \boldsymbol{\Delta}\right)\boldsymbol{T}_{BI}\boldsymbol{E}\right] \times \boldsymbol{h}_d\right\} \tag{26}$$

where $\boldsymbol{T}_{BI}$ is the coordinate transformation matrix between $\mathbb{F}_I$ and $\mathbb{F}_B$, $\boldsymbol{Z} = \boldsymbol{T}_{BI}^T\boldsymbol{\zeta}$, and $\boldsymbol{E} = \boldsymbol{T}_{BI}^T\boldsymbol{\varepsilon}$. Given $\boldsymbol{Y} = \left(\boldsymbol{Z}^T, \boldsymbol{E}^T\right)^T$, $\boldsymbol{Y} \in \mathbb{R}^6$, the system in Eqs. (25) and (26) achieves the form

$$\dot{\boldsymbol{Y}} = -\boldsymbol{A}(t)\boldsymbol{K}\,\boldsymbol{Y} - \boldsymbol{B}\,(t, \boldsymbol{Y}) - \boldsymbol{C}\,(t, \boldsymbol{Y}) \tag{27}$$

where

$$\boldsymbol{A}(t) = \begin{pmatrix} \boldsymbol{T}_{BI}^T\left(\boldsymbol{I}_3 - \hat{\boldsymbol{b}}\,\hat{\boldsymbol{b}}^T\right)\boldsymbol{T}_{BI} & \boldsymbol{T}_{BI}^T\left(\boldsymbol{I}_3 - \hat{\boldsymbol{b}}\,\hat{\boldsymbol{b}}^T\right)\boldsymbol{T}_{BI} \\ \boldsymbol{T}_{BI}^T\left(\boldsymbol{I}_3 - \hat{\boldsymbol{b}}\,\hat{\boldsymbol{b}}^T\right)\boldsymbol{T}_{BI} & \boldsymbol{T}_{BI}^T\left(\boldsymbol{I}_3 - \hat{\boldsymbol{b}}\,\hat{\boldsymbol{b}}^T\right)\boldsymbol{T}_{BI} \end{pmatrix} \in \mathbb{R}^{6\times 6} \tag{28}$$

is a time-dependent matrix,

$$\boldsymbol{K} = \begin{pmatrix} k_\zeta \boldsymbol{I}_3 & \boldsymbol{0}_{3\times 3} \\ \boldsymbol{0}_{3\times 3} & k_\varepsilon \boldsymbol{I}_3 \end{pmatrix} \in \mathbb{R}^{6\times 6} \tag{29}$$

is a gain matrix, and

$$\boldsymbol{B}(t,\boldsymbol{Y}) = \begin{pmatrix} \boldsymbol{0}_{3\times 1} \\ \boldsymbol{T}_{BI}^T \left[\left(\boldsymbol{J}_a^{-1} \boldsymbol{T}_{BI} \boldsymbol{E} \right) \times \boldsymbol{h}_d \right] \end{pmatrix}, \quad \boldsymbol{C}(t,\boldsymbol{Y}) = \begin{pmatrix} \boldsymbol{0}_{3\times 1} \\ \boldsymbol{T}_{BI}^T \left[\left(\boldsymbol{\Delta T}_{BI} \boldsymbol{E} \right) \times \boldsymbol{h}_d \right] \end{pmatrix} \tag{30}$$

are gyroscopic coupling terms.

Equation (27) matches the classical formulation of a perturbed system $\dot{\boldsymbol{Y}} = \boldsymbol{f}(t,\boldsymbol{Y}) + \boldsymbol{g}(t,\boldsymbol{Y})$ where $\boldsymbol{f}(t,\boldsymbol{Y}) = -\boldsymbol{A}(t)\boldsymbol{K}\,\boldsymbol{Y} - \boldsymbol{B}(t,\boldsymbol{Y})$ governs the nominal system and $\boldsymbol{g}(t,\boldsymbol{Y}) = -\boldsymbol{C}(t,\boldsymbol{Y})$ is a vanishing perturbation term, $\boldsymbol{g}(t,\boldsymbol{0}) = \boldsymbol{0}$. Global exponential stability is addressed by the following Lemma.

Lemma 1 *Consider the nonlinear perturbed time-varying system defined by Eqs.* (27)-(30) *and let* $\bar{\gamma} = |h_d|\,\delta_{\max}$, *where* $\delta_{\max} = \max\{|\delta_1|, |\delta_2|, |\delta_3|\}$. *If* $\bar{\gamma}$ *is sufficiently small, then the origin* $\boldsymbol{Y} = \boldsymbol{0}$ *is globally exponentially stable.*

Proof: See Appendix. □

Remark 1: According to the factorization chosen for the gyroscopic coupling terms in Eq. (30), one has

$$\delta_{\max} = \frac{|J_1 - J_3|}{\min\{J_1, J_3\}\ (J_1 + J_3)}. \tag{31}$$

The bound on $\bar{\gamma}$ thus translates into a requirement on the maximum magnitude of the desired wheel spin rate, actually relaxed when the moments of inertia about the transverse axes are sufficiently close to each other (thus approaching the case when the satellite has axisymmetric inertia properties). This is a likely scenario for many practical applications dealing with small-scale spacecraft, where almost cubic or cylindrical oblate configurations are typically employed. Unfortunately, it is not always possible to quantitatively evaluate a bound for $\bar{\gamma}$, in which case robustness is proven only at a qualitative level. Even though a bound on $\bar{\gamma}$ represents an additional piece of information, one should not overemphasize its relevance, as it may result into conservative estimates for the perturbation $\boldsymbol{g}(t,\boldsymbol{Y}) = -\boldsymbol{C}(t,\boldsymbol{Y})$, if obtained from the analysis of a worst case scenario.

Remark 2: Note that if the satellite possesses exactly an axisymmetric matrix of inertia with respect to the pitch axis, then $\boldsymbol{C}(t, \boldsymbol{Y}) = \boldsymbol{0}$ and $\bar{\gamma} = 0$. In this particular case, global exponential stability is inferred by the first part of the Proof of Lemma 1 in the Appendix.

Remark 3: The system dynamics described by Eq. (27) cannot be addressed without taking into account the attitude of the spacecraft, affecting $\boldsymbol{B}(t, \boldsymbol{Y})$ and $\boldsymbol{C}(t, \boldsymbol{Y})$ through the matrix $\boldsymbol{T}_{BI}$. Nonetheless, such consideration does not hold for the proof of stability discussed in the Appendix. In fact, the presence of the attitude matrix only affects the evolution in time of the terms $\boldsymbol{B}(t, \boldsymbol{Y})$ and $\boldsymbol{C}(t, \boldsymbol{Y})$, influencing the rate of convergence toward the equilibrium, without any consequence on the asymptotic behavior of the closed-loop system.

Lemma 1 demonstrates that the dynamics introduced in Eqs. (25) and (26) drives the error variables $\boldsymbol{E}$ and $\boldsymbol{Z}$ asymptotically to zero. This stability property is invariant with respect to the frame in which vectors are expressed. In other words, $\boldsymbol{\zeta}$ and $\boldsymbol{\varepsilon}$ also approach null vectors asymptotically. Consequently, by Eq. (20), also $\boldsymbol{M}^{(c)}(t) \to 0$ as $t \to \infty$. From Eq. (23), the components of $\boldsymbol{\varepsilon}$ are given by

$$\boldsymbol{\varepsilon} = \begin{pmatrix} 0 \\ h_d \\ 0 \end{pmatrix} - \begin{pmatrix} 0 \\ h \\ 0 \end{pmatrix} - \begin{pmatrix} J_1\omega_1 \\ J_2\omega_2 \\ J_3\omega_3 \end{pmatrix} \tag{32}$$

such that, when $\boldsymbol{\varepsilon} \to \boldsymbol{0}$, then

$$\omega_1, \omega_3 \to 0, \quad h + J_2\omega_2 \to h_d \tag{33}$$

Provided $\boldsymbol{H}_d = h_d\hat{\boldsymbol{\sigma}}$, where $\hat{\boldsymbol{\sigma}} = \boldsymbol{T}_{BO}\,(0,1,0)^T$, and taking into account the formulation of the attitude matrix in Eq. (4), it is

$$\boldsymbol{H}_d = h_d \begin{pmatrix} \cos\theta\sin\psi + \sin\phi\sin\theta\cos\psi \\ \cos\phi\cos\psi \\ \sin\theta\sin\psi - \sin\phi\cos\theta\cos\psi \end{pmatrix} \tag{34}$$

Since also $\boldsymbol{\zeta} \to \mathbf{0}$, then

$$h_d \left(\cos\theta \sin\psi + \sin\phi \sin\theta \cos\psi\right) - J_1\omega_1 \to 0 \tag{35}$$

$$h_d \cos\phi \cos\psi - (h + J_2\omega_2) \to 0 \tag{36}$$

$$h_d \left(\sin\theta \sin\psi - \sin\phi \cos\theta \cos\psi\right) - J_3\omega_3 \to 0 \tag{37}$$

Furthermore, by considering the limits in Eq. (33), one obtains:

$$\cos\theta \sin\psi + \sin\phi \sin\theta \cos\psi \to 0 \tag{38}$$

$$\cos\phi \cos\psi \to 1 \tag{39}$$

$$\sin\theta \sin\psi - \sin\phi \cos\theta \cos\psi \to 0 \tag{40}$$

It follows from Eq. (39) that $\cos\phi \to \pm 1$ and $\cos\psi \to \pm 1$ and thus $\lim_{t\to+\infty} \cos\phi = \lim_{t\to+\infty} \cos\psi$, with the limits having the same sign. Also $\sin\phi$, $\sin\psi \to 0$, which is possible only if the pitch axis becomes aligned, as required, with the direction $\hat{\boldsymbol{\sigma}}$, normal to the orbit plane.

C. Control of the Pitch Angle

The equation governing the dynamics of the spacecraft around the pitch axis is derived from Eq. (1), namely

$$J_2\,\dot{\omega}_2 + (J_1 - J_3)\,\omega_1\omega_3 = -\dot{h} + M_2^{(c)} \tag{41}$$

Taking $\dot{h}$ as the control input defined in Eq. (21) and introducing the error on the body frame pitch angular rate, $\xi = n - \omega_2$, Eq. (41) becomes:

$$\dot{\tilde{\xi}} + k\,\tilde{\xi} = d \tag{42}$$

where $\tilde{\xi} = \lambda\theta - \xi$ is a filtered pitch error and $d = \left[-(J_1 - J_3)\,\omega_1\omega_3 + M_2^{(c)}\right]/J_2$ represents a disturbance term.

Since Lemma 1 guarantees the exponential stability of the origin $\boldsymbol{Y} = \mathbf{0}$ of the system in Eqs. (27)-(30), there exists a time instant $\bar{t} \geq t_0$ such that all the quantities $|\omega_1|$, $|\omega_3|$, $|\sin\psi|$, and $|\sin\phi|$ become smaller than a prescribed threshold for all $t \geq \bar{t}$. Thus, the system in Eq. (42) with $k > 0$ is an asymptotically stable linear time-invariant system driven by an asymptotically vanishing

disturbance d and it is possible to conclude that $\tilde{\xi} \to 0$ as $t \to \infty$. From the definition of the filtered error, $\tilde{\xi}$, and by considering Eq. (9), it is:

$$\tilde{\xi} = \lambda\,\theta - n + \dot{\theta} + \dot{\psi}\,\sin\phi + n\,\cos\phi\cos\psi \to 0 \tag{43}$$

for $t \to \infty$. Since $\dot{\psi}$, $\sin\phi \to 0$ and $\cos\phi\cos\psi \to 1$, it follows that

$$\dot{\theta} + \lambda\,\theta \to 0 \tag{44}$$

Let

$$\dot{\theta} + \lambda\,\theta = \bar{r} \tag{45}$$

By Eq. (44), $\bar{r} \to 0$. Since Eq. (45) is an asymptotically stable linear time-invariant system driven by an asymptotically vanishing disturbance $\bar{r} \to 0$, it can be finally concluded that $\dot{\theta}$, $\theta \to 0$.

Note that if $\tilde{\xi} \to 0$ and $\theta \to 0$ also $\xi = n - \omega_2 \to 0$ as $t \to \infty$. In other words, the spacecraft is driven to perfect alignment with the orbit frame and rotates about the pitch axis with n angular rate with respect to the inertial frame. From Eq. (33) it thus follows that the remaining angular momentum stored in the spacecraft is obtained by the spinning of the MW with respect to the body frame with the desired rate Ω_d.

Remark 4: As previously mentioned, the 3-1-2 Euler sequence determines a singularity at $\phi = \pm 90$ deg in Eqs. (11) and (13). For practical control implementation purposes, a discussion was already presented in Section II.B. From a mathematical standpoint, this implies that the pitch angle stabilization proof holds almost globally.

IV. Results and Discussion

The control laws proposed in Section III.A for the attitude stabilization of a spacecraft and the acquisition of a desired spin rate on the MW are applied to a LEO micro-satellite, equipped with three mutually orthogonal MTs. Table 1 shows relevant spacecraft data and orbit parameters, together with initial conditions for a sample maneuver.

A nonlinear model for spacecraft attitude dynamics is used in the simulations, where numerical propagation of Euler parameters is performed [13]. No friction is considered for the wheel assembly,

Table 1 Spacecraft and orbit data, with initial conditions for a sample maneuver.

Parameter	Symbol	Value	Units
Spacecraft data			
Principal moments of inertia	$J_1,\ J_2,\ J_3$	2.023, 2.060, 0.865	kg m^2
Wheel moment of inertia	J_w	4.20×10^{-4}	kg m^2
Maximum magnetic dipole	$m_{\max}$	3.5	A m^2
Maximum wheel torque	$g_{\max}$	0.01	N m
Orbit data			
Radius	r_c	6 905	km
Period	T	5710	s
Inclination	i	97	deg
Sample maneuver			
Initial Conditions	$\boldsymbol{\omega}_0$	$(0,\ 0.1761,\ 0)^T$	rad/s
	$\psi_0,\ \phi_0,\ \theta_0$	$18.2, 21.8, -14.2$	deg

so that g is the control input for the pitch control law. The initial phase during which the satellite is magnetically detumbled after injection into its orbit is not analyzed here, as it is not relevant in the framework of the present study. It is assumed that, after the initial detumbling phase [14, 15], the spacecraft lies in a pure spin condition about its pitch axis with a total angular momentum $||\boldsymbol{J}\,\boldsymbol{\omega}_0 + \boldsymbol{h}_0|| = 1.2\,h_d$, 20% larger than the desired one, $h_d = J_2\,n + J_w\,\Omega_d = 0.3023$ Nms, provided $J_w\,\Omega_d = 0.3$ Nms. The wheel is at rest relative to the body axes at time t_0, namely $\boldsymbol{h}_0 = \boldsymbol{0}$ Nms. The initial direction of the pitch axis is tilted 30 deg away from the orbit normal. During the controlled maneuver, the excess of angular momentum is expected to be dissipated by MTs and, at the same time, the residual angular momentum is distributed between the spacecraft and the wheel, the latter term increasing to its desired value of 0.3 Nms. The gains for the magnetic control law are selected as [9] $k_\zeta = k_\varepsilon = 0.004$ s^{-1}, whereas the gains for the wheel control law are $k = 0.1$ s^{-1} and $\lambda = 0.1$ rad^{-1}s^{-1}.

In the first simulation (Case 1), no external disturbance is applied to the spacecraft and it is assumed that spacecraft body frame is a principal-axis frame, that is, $\boldsymbol{J} = \boldsymbol{J}^*$ is a diagonal matrix.

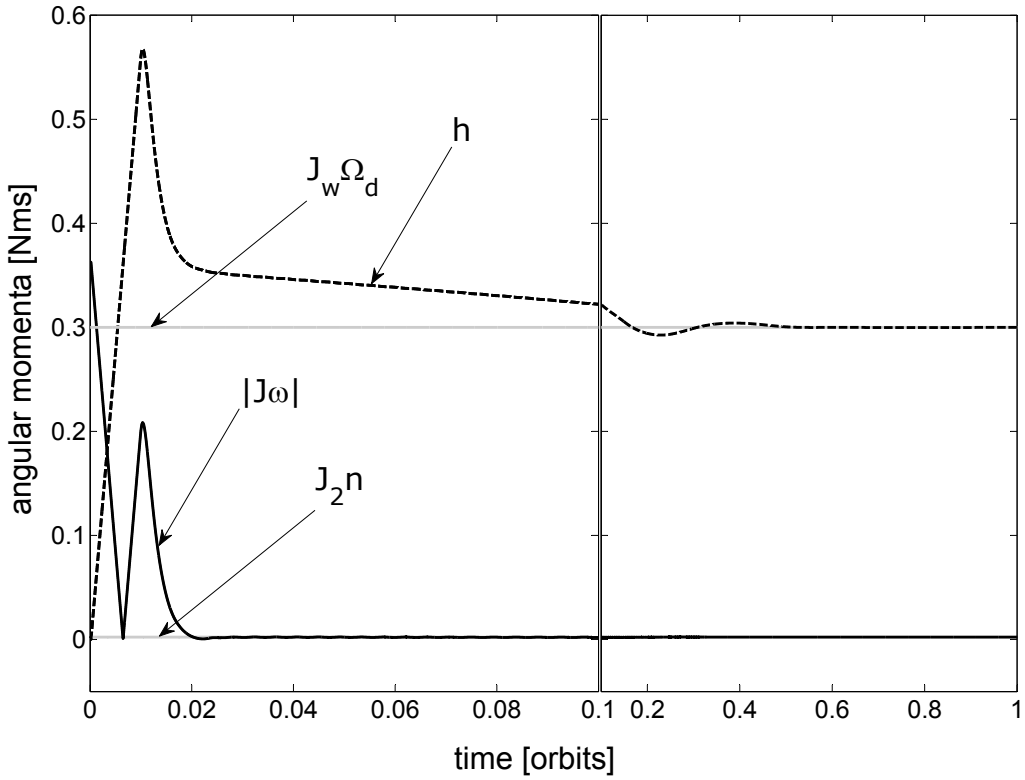

Figure 2 Spacecraft and wheel angular momenta (Case 1).

Time histories of angular momenta are reported in Fig. 2, where $\boldsymbol{J}\,\boldsymbol{\omega}$ converges to the desired value, $\boldsymbol{J}\,\boldsymbol{\omega}^{orb}$, while pitch-axis pointing is performed along the orbit normal, with the "yaw" and "roll" angles, ψ and ϕ (that is, azimuth and elevation of the pitch axis with respect to the orbit plane, respectively), approaching zero (Fig. 3). Figure 4 shows that the MTs initially saturate when the errors are large. At the same time, pitch control torque distributes the angular momentum between spacecraft and MW, driving the body frame to three-axis stabilization with respect to the orbit frame and the wheel to the desired spin condition with respect to the spacecraft, namely $h \to J_w\,\Omega_d$ in about 1 orbit. In particular, the pitch angle θ rapidly converges to zero as predicted by Eq. (45), where disturbance $\bar{r}$, significantly affecting only the very initial portion of the maneuver (approximately 0.01 orbits), vanishes as $t \to \infty$.

In the second test case (Case 2), starting from the same initial conditions, gravity gradient, aerodynamic, and residual magnetic torques are included in the model in order to test robustness of the closed-loop system with respect to external disturbances. In particular, the aerodynamic torque

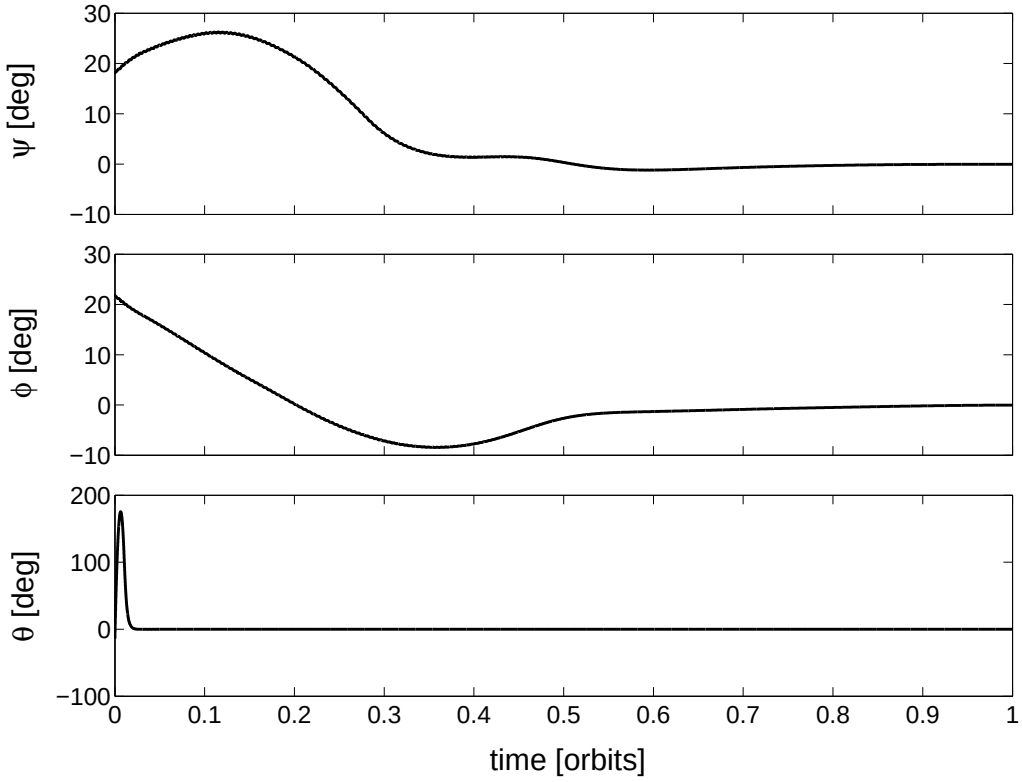

Figure 3 Spacecraft attitude error (Case 1).

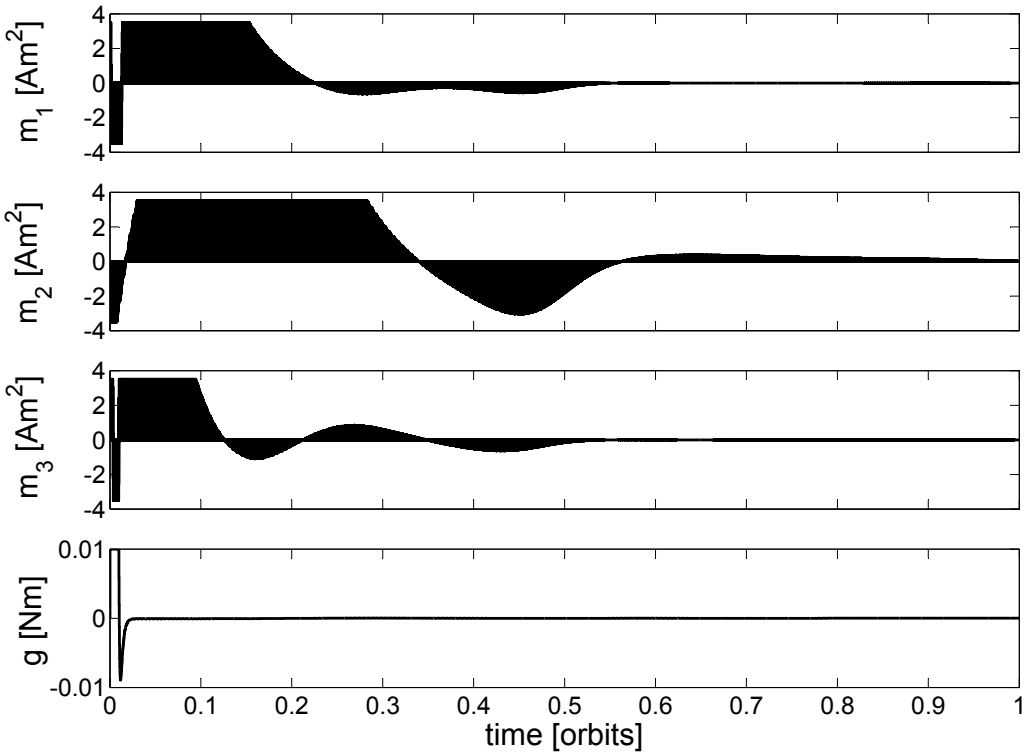

Figure 4 Magnetorquers and wheel efforts (Case 1).

described by Eqs. (15) and (16) is characterized by the air density $\rho = 6.39 \cdot 10^{-13}$ kg/m^3 at the considered orbit altitude and a drag coefficient C_D =2.2 is assumed for a parallelepiped micro-satellite with dimensions 0.3 × 0.3 × 0.6 m. A residual magnetic dipole $\boldsymbol{m}_{rm} = (0.1, 0.1, 0.1)^T$ Am^2 affects spacecraft actuation performance. Zero-mean Gaussian white noise is added to each Euler angle and angular velocity measurement, with standard deviation 1.07 deg and 0.01 deg/s, respectively, for simulating the effects of sensor noise. Analogous modeling is performed for magnetometer measurement noise on each axis, with standard deviation equal to 3 nT. The generated control signals are finally sampled at a frequency of 1 Hz and are compatible with the current technology of commercial MTs [3].

To further demonstrate robustness also in the presence of off-diagonal terms in the spacecraft inertia matrix, the spacecraft principal axes are offset from the spacecraft body axes and principal moments of inertia are varied with respect to their nominal values used for $\boldsymbol{J}^*$. This simulates both misalignment of sensor and control axes with respect to their nominal direction and uncertainties on the knowledge of mass distribution for the spacecraft. A perturbed inertia matrix $\boldsymbol{J}$ is thus considered in Case 2, where

$$\boldsymbol{J} = \begin{pmatrix} 1.9384 & 0.0134 & -0.0016 \\ 0.0134 & 2.0861 & -0.0286 \\ -0.0016 & -0.0286 & 0.8939 \end{pmatrix}$$

The corresponding principal moments of inertia are given by $\boldsymbol{J}_P^* = \text{diag}(1.9372, 2.0880, 0.8932)$.

Figures 5, 6, and 7 show the results of the second simulation (Case 2), where time histories of both angular momenta of the spacecraft and attitude variables are similar to those obtained for Case 1 in the first phase of the maneuver, when momentum management takes place. In steady state conditions, the error variables remain bounded in the presence of non-modeled disturbances.

The enlargements in Fig. 6 shows the oscillation on attitude angles, which remain bounded within a few tenths of a degree. Precision on pitch angle proved to be the most critical aspect, at least for the considered set of perturbations, pitch error reaching peak values higher than 0.5 deg. Nonetheless, Euler angles and angular rates of the spacecraft with respect to the orbit frame oscillate with a pointing accuracy of approximately 0.25 deg and 0.02 deg/s, respectively, on each

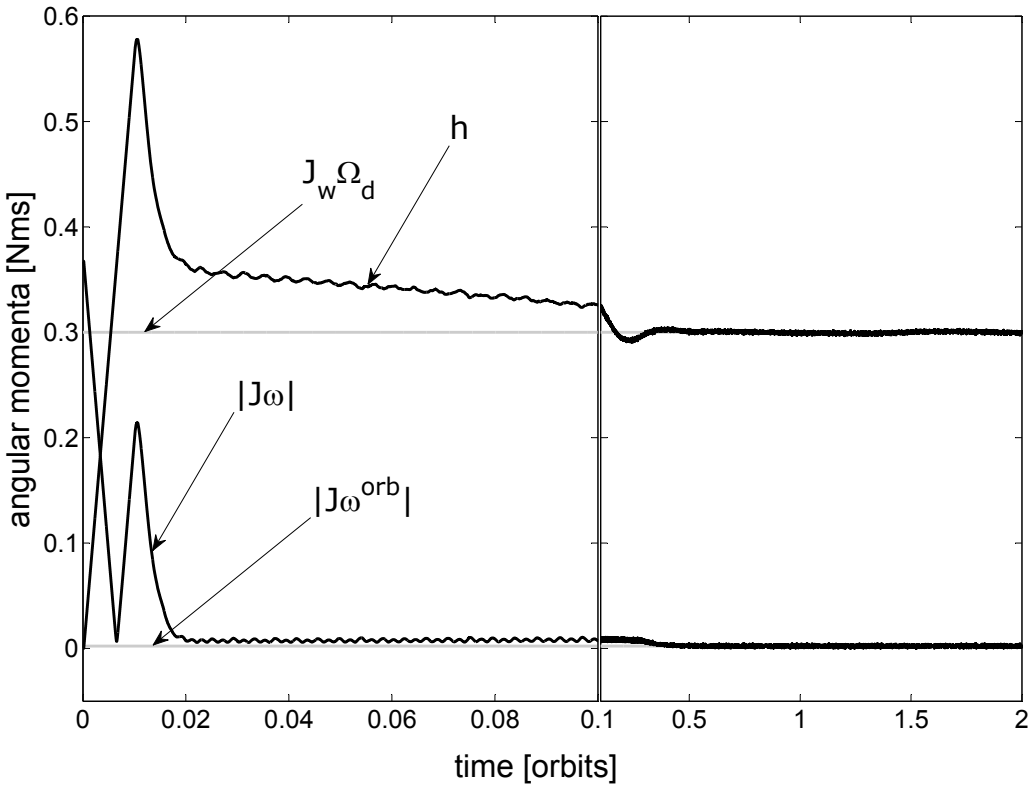

Figure 5 Spacecraft and wheel angular momenta (Case 2).

axis in terms of standard deviation. Statistical analysis is performed over 20 orbits in steady state conditions, which also practically demonstrates long term stability of the whole system.

Such a performance is obtained at the expenses of a rather intense control action. If a comparison between Figs. 4 and 7 is performed, one immediately notes that all command variables decrease asymptotically to 0, whereas a large control effort is present, especially for momentum dipole m_2, but also for the MW command torque g. Finally, the enlargement reported in the time-history of m_1 shows that, in this more realistic scenario, the magnetorquers are activated with a frequency of 1 Hz. In spite of uncertainties, disturbances, saturation, quantization and piece-wise constant control action, the behavior of the closed loop system remains satisfactory.

V. Conclusions

A proof of convergence is derived for magnetic and mechanical control laws that drive a rigid spacecraft to attitude stabilization in the orbit frame by means of three mutually orthogonal mag-

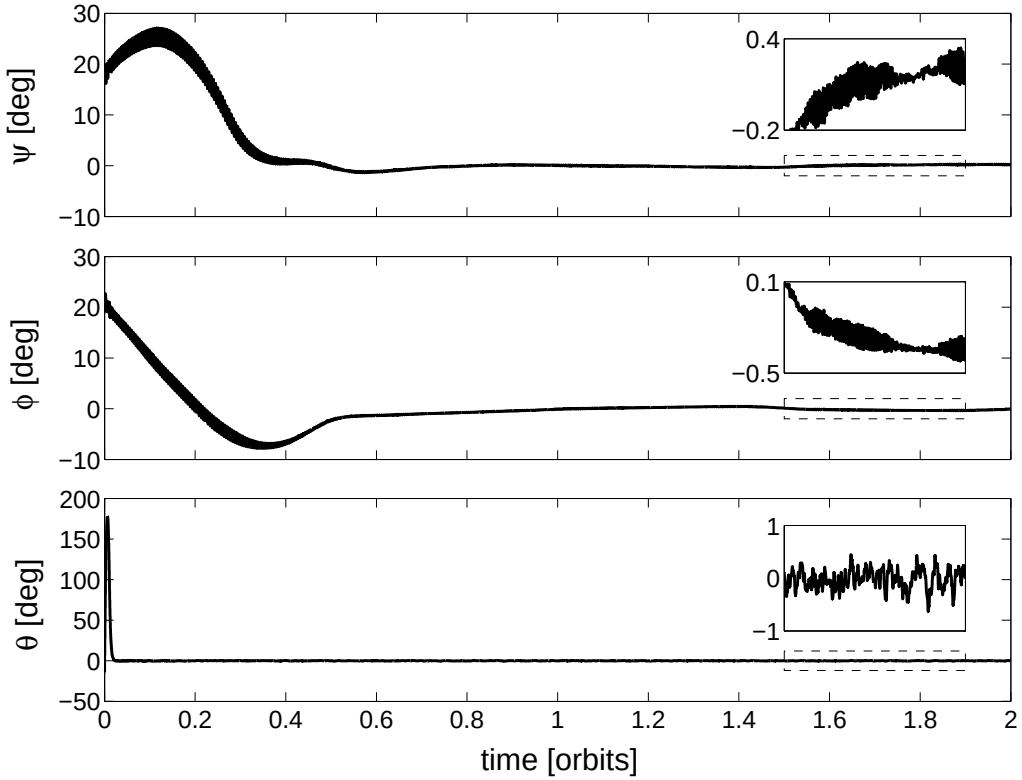

Figure 6 Spacecraft attitude error (Case 2).

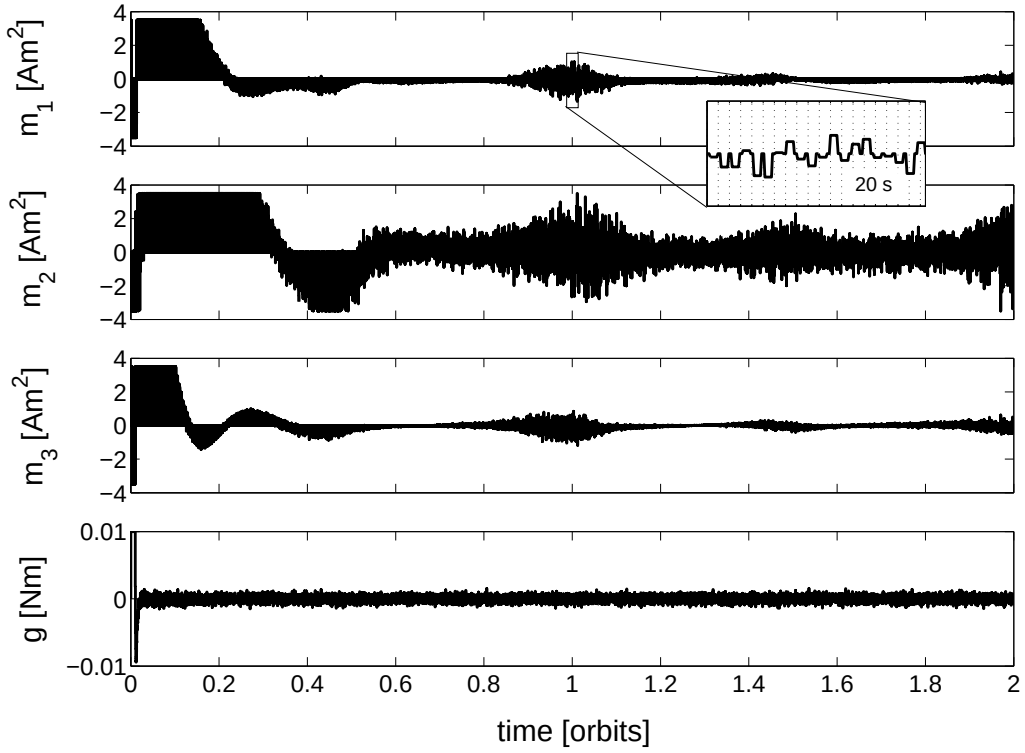

Figure 7 Magnetotorquers and wheel efforts (Case 2).

netic actuators and a momentum wheel with spin axis parallel to the pitch axis. The stability proof is obtained under the assumption that a set of principal axes of inertia is selected as the body-fixed frame. This proof extends a method developed for the acquisition of a pure spin around a principal axis of inertia, while aiming the spin axis in a desired inertially-fixed direction. In particular, global exponential stability is proven for the closed-loop system where angular momentum management is obtained by means of magnetic actuation. The pitch angle convergence proof, which represents the additional contribution of the present paper, immediately follows after a proper choice of the wheel control law. The variability of the magnetic field along the orbit plays an important role in the proof of asymptotic stability of the system towards the equilibrium point. The results hold for many practical applications regarding small-scale spacecraft, where almost cubic or cylindrical oblate configurations are typically employed.

Simulation results are presented in order to demonstrate the effectiveness of the control laws and validate the theoretical results. As a further contribution, the control laws are shown to perform well in the presence of external disturbances, spacecraft inertia matrix uncertainties, and control implementation issues such as actuator saturation, control quantization, and measurement noise.

Appendix: Proof of Lemma 1

First the proof of exponential stability of $\boldsymbol{Y} = \boldsymbol{0}$ is addressed in the case when $\bar{\gamma} = 0$. In such framework, the system in Eqs. (27)-(30) assumes the following structure:

$$\dot{\boldsymbol{Y}} = -\boldsymbol{A}(t)\boldsymbol{K}\,\boldsymbol{Y} - \boldsymbol{B}\,(t, \boldsymbol{Y}) \tag{46}$$

Let

$$V(\boldsymbol{Y}) = 1/2\,\boldsymbol{Y}^T\boldsymbol{K}\boldsymbol{Y} \tag{47}$$

be a Lyapunov function candidate. Provided $\nabla_Y V$ is the gradient of V along the trajectories of the considered system, it is

$$\dot{V}(t, \boldsymbol{Y}) \equiv (\nabla_Y V)^T\ \boldsymbol{f}(t, \boldsymbol{Y}) = -\,(\boldsymbol{K}\boldsymbol{Y})^T\,\boldsymbol{A}(t)\,(\boldsymbol{K}\boldsymbol{Y}) \tag{48}$$

where $\boldsymbol{A}(t)$ is a positive semi-definite matrix. In what follows, it is proven that V and its time-derivative $\dot{V}$ satisfy the hypotheses of Theorem 8.5 in Ref. [17]. In particular, $V(\boldsymbol{Y})$ is continuously

differentiable and $\dot{V}(t, \boldsymbol{Y})$ is uniformly continuous and negative semi-definite.

From Eq. (48), the time-derivative of $V(t, \boldsymbol{Y})$ vanishes if one of the following conditions holds:

a) the equilibrium point at the origin is reached, $(\boldsymbol{Z}^T, \boldsymbol{E}^T)^T = \boldsymbol{0}$ or

b) the angular momentum error variables are such that the error signal, $\boldsymbol{e} = k_\zeta \, \boldsymbol{Z} + k_\varepsilon \, \boldsymbol{E}$, becomes parallel to the Earth magnetic field (and the nominal torque $\boldsymbol{M}^{(c)}$ thus vanishes) or

c) the linearly independent angular momentum error variables are such that the error signal, $\boldsymbol{e} = k_\zeta \, \boldsymbol{Z} + k_\varepsilon \, \boldsymbol{E}$, becomes null with $\boldsymbol{Z} \neq \boldsymbol{0}$, $\boldsymbol{E} \neq \boldsymbol{0}$ (and the nominal torque $\boldsymbol{M}^{(c)}$ again vanishes).

In the case of torque-free motion (Conditions b and c), the nominal system (46) reduces to $\dot{\boldsymbol{Y}} = -\boldsymbol{B}\,(t, \boldsymbol{Y})$. Taking into account the definition of the term $\boldsymbol{B}\,(t, \boldsymbol{Y})$ in Eq. (30), this means that $\boldsymbol{Z}$ remains fixed in the inertial frame.

Suppose Condition b holds. This situation can be maintained over time if and only if the vector $(k_\zeta \boldsymbol{Z}^T, k_\varepsilon \boldsymbol{E}^T)^T$ remains in the null-space of the time varying matrix, $\boldsymbol{A}(t)$, $\mathcal{N}_A = \ker(\boldsymbol{A})$. Letting $\boldsymbol{0} = (0, 0, 0)^T$, a basis for the null-space of $\boldsymbol{A}$ is given by the vectors $\boldsymbol{n}_1 = (\boldsymbol{b}^T, \boldsymbol{0}^T)^T$, $\boldsymbol{n}_2 = (\boldsymbol{0}^T, \boldsymbol{b}^T)^T$, $\boldsymbol{n}_3 = (\boldsymbol{u}^T, -\boldsymbol{u}^T)^T$, and $\boldsymbol{n}_4 = (\boldsymbol{v}^T, -\boldsymbol{v}^T)^T$, where $\boldsymbol{u}$ and $\boldsymbol{v}$ are a pair of linearly independent vectors perpendicular to $\boldsymbol{b}$. The vector $(k_\zeta \boldsymbol{Z}^T, k_\varepsilon \boldsymbol{E}^T)^T \in \mathcal{N}_A$ if $k_\zeta \boldsymbol{Z}$ and $k_\varepsilon \boldsymbol{E}$ have components opposite in sign on the plane perpendicular to $\boldsymbol{b}$, which means that the three vectors $k_\zeta \boldsymbol{Z}$, $k_\varepsilon \boldsymbol{E}$, and $\boldsymbol{b}$ must belong to the same plane. Such a condition can be reached, but it cannot be maintained over a finite time-interval during a torque-free phase, since the error signal $\boldsymbol{e}$ rotates about the inertially-fixed direction of $\boldsymbol{Z}$. But this is in contrast with the motion of $\boldsymbol{b}$ in the inertial frame, as described by the IGRF model.

Now suppose Condition c holds. The error signals, $\boldsymbol{Z}$ and $\boldsymbol{E}$, are such that $k_\zeta \, \boldsymbol{Z} = -k_\varepsilon \, \boldsymbol{E}$, with the result that, during the torque-free motion, both $\boldsymbol{Z}$ and $\boldsymbol{E}$ remain fixed in the inertial frame. Considering the definition of the momentum error vector $\boldsymbol{E}$ in Eq. (19), this means that $\boldsymbol{h}_d$ does not move in the inertial space too, being the total momentum vector fixed during a torqueless condition. This situation may occur in two cases: 1) the spacecraft spins about the prescribed principal axis of inertia, namely $\boldsymbol{T}_{BI}\boldsymbol{E} \times \boldsymbol{h}_d = \boldsymbol{0}$, while the spin axis aims in the direction of the orbit normal; as a

matter of fact, this situation is in contrast, when $\boldsymbol{E} \neq \boldsymbol{0}$, with the condition $\dot{\boldsymbol{Y}} = -\boldsymbol{B}\,(t, \boldsymbol{Y}) = \boldsymbol{0}$, that implies $\left(\boldsymbol{J}_a^{-1}\boldsymbol{T}_{BI}\boldsymbol{E}\right) \times \boldsymbol{h}_d = \boldsymbol{0}$; 2) in case the satellite is in a rest condition, then $\|\boldsymbol{Z}\| = \|\boldsymbol{E}\| = |h_d|$; the situation $k_\zeta\,\boldsymbol{Z} = -k_\varepsilon\,\boldsymbol{E}$ can thus be avoided by choosing $k_\zeta \neq k_\varepsilon$.

Given the above considerations, the origin $\boldsymbol{Y} = \boldsymbol{0}$ is globally asymptotically stable and the right-hand term of the equation

$$V(\boldsymbol{Y}(t+\delta)) - V(\boldsymbol{Y}(t)) = \int_t^{t+\delta} (\nabla_Y V)^T\ \boldsymbol{f}(s, \boldsymbol{Y}(s))\,ds = -\int_t^{t+\delta} (\boldsymbol{K}\boldsymbol{Y})^T\,\boldsymbol{A}(s)\,(\boldsymbol{K}\boldsymbol{Y})\ ds \tag{49}$$

is a finite negative term if an equilibrium point is not reached, provided $\delta > 0$ is a finite time interval. As a last element to infer global exponential stability, it is necessary to demonstrate that, for $V(t) = V[\boldsymbol{Y}(t)]$, for some δ over $t \geq t_0$, the inequality

$$V(t+\delta) - V(t) \leq -\lambda V(t) \tag{50}$$

holds uniformly in the time domain for a positive constant λ. Since $\dot{V}$ can become zero, but constant V surfaces do not contain solutions (see above), one expects that those time instants $t^\star$ when $\boldsymbol{A}(t^\star)\boldsymbol{K}\boldsymbol{Y}^\star = \boldsymbol{0}$ and $\dot{V} = 0$ are inflection points with horizontal tangent for the time-history $V(t) = V\,[\boldsymbol{Y}(t)]$, with $\ddot{V} = 0$ for $t = t^\star$ and $\dot{V} < 0$ immediately before and after $t^\star$. Provided V is continuously differentiable, from the properties of inflection points with horizontal tangent it follows [18]

$$V(t+\delta) - V(t) \leq V(t^\star + \delta) - V(t^\star) < 0 \tag{51}$$

for a sufficiently small δ and all $t \geq t_0$. By expanding $V(t)$ in terms of a Taylor series up to the third order, where

$$V(t+\delta) - V(t) = \dot{V}(t)\delta + (1/2!)\ddot{V}(t)\delta^2 + (1/3!)\dddot{V}(t)\delta^3 + \mathcal{O}(\delta^4)$$

for $t = t^\star$ one has:

$$V(t^\star + \delta) - V(t^\star) = (1/6)\dddot{V}(t^\star)\delta^3 + \mathcal{O}(\delta^4) \tag{52}$$

Thus, in order to satisfy the last requirement for global stability of the origin, it is necessary to prove that the dominant term $\dddot{V}(t^\star)$ on the right-hand-side of Eq. (52) is always negative and finite

for all those time instants $t^\star$ when $\dot{V} = 0$ (hence $\ddot{V} = 0$), in order to use $\dddot{V}$ for estimating the candidate λ in the neighborhood of $t^\star$ to be employed in Eq. (50).

From Eqs. (46), (47), and (48), one gets that, for the particular case proposed in the present paper, when $\dot{V} = 0$, it is $\boldsymbol{A}(t)\boldsymbol{KY} = \boldsymbol{0}$, that is the vector $\boldsymbol{KY}$ lies on the null space of $\boldsymbol{A}$. The second time-derivative of V,

$$\ddot{V}(t, \boldsymbol{Y}) = -2\left(\boldsymbol{KY}\right)^T \boldsymbol{A}(t) \left(\boldsymbol{K}\dot{\boldsymbol{Y}}\right) - \left(\boldsymbol{KY}\right)^T \dot{\boldsymbol{A}}(t) \left(\boldsymbol{KY}\right)$$

is also zero for $t = t^\star$ if and only if the null space of $\dot{\boldsymbol{A}}(t^\star)$ coincides with or contains the null space of $\boldsymbol{A}(t^\star)$. The expression of the third time-derivative of V,

$$\begin{aligned}\dddot{V}(t, \boldsymbol{Y}) = &-4\left(\boldsymbol{KY}\right)^T \boldsymbol{A}(t) \left(\boldsymbol{K}\ddot{\boldsymbol{Y}}\right) - 2\left(\boldsymbol{K}\dot{\boldsymbol{Y}}\right)^T \boldsymbol{A}(t) \left(\boldsymbol{K}\dot{\boldsymbol{Y}}\right) - 2\left(\boldsymbol{KY}\right)^T \dot{\boldsymbol{A}}(t) \left(\boldsymbol{K}\dot{\boldsymbol{Y}}\right) \\ &- 2\left(\boldsymbol{KY}\right)^T \dot{\boldsymbol{A}}(t) \left(\boldsymbol{K}\dot{\boldsymbol{Y}}\right) - \left(\boldsymbol{KY}\right)^T \ddot{\boldsymbol{A}}(t) \left(\boldsymbol{KY}\right)\end{aligned}$$

for $t = t^\star$ is thus reduced to

$$\dddot{V}(t^\star, \boldsymbol{Y}^\star) = J_{\ddot{\boldsymbol{A}}} + J_{\boldsymbol{B}} = -\left(\boldsymbol{KY}^\star\right)^T \ddot{\boldsymbol{A}}(t^\star) \left(\boldsymbol{KY}^\star\right) - 2\left(\boldsymbol{KB}^\star\right)^T \boldsymbol{A}(t^\star) \left(\boldsymbol{KB}^\star\right) \tag{53}$$

where $\boldsymbol{B}^\star = \boldsymbol{B}(t^\star, \boldsymbol{Y}^\star)$. The third time derivative of the candidate Lyapunov function depends on the sum of two negative semi-definite quadratic forms, $J_{\ddot{\boldsymbol{A}}}$ and $J_{\boldsymbol{B}}$. If one proves that at least one of the two terms is strictly negative when $\dot{V} = 0$, the third time derivative of V is strictly negative at $t = t^\star$ and it is possible to derive a finite value of λ that satisfies the inequality in Eq. (50).

The null space of $\boldsymbol{A}$ can be decomposed into the Cartesian product of two subspaces, $\mathcal{N}_A = \mathcal{N}_1 \times \mathcal{N}_2$, with $\mathcal{N}_1 = \text{span}\{(\hat{\boldsymbol{b}}^T, \boldsymbol{0}^T)^T, (\boldsymbol{0}^T, \hat{\boldsymbol{b}}^T)^T\}$, and $\mathcal{N}_2 = \text{span}\{(\boldsymbol{u}^T, -\boldsymbol{u}^T)^T, (\boldsymbol{v}^T, -\boldsymbol{v}^T)^T\}$. It is possible to show that, when $\boldsymbol{KY} \in \mathcal{N}_1$, that is, both errors $\boldsymbol{Z}$ and $\boldsymbol{E}$ are parallel to the geomagnetic field vector, $\hat{\boldsymbol{b}}$, the term $J_{\ddot{\boldsymbol{A}}}$ is strictly negative for $t = t^\star$. This is proved assuming initially $\boldsymbol{E} = \|\boldsymbol{E}\|\hat{\boldsymbol{b}}$ and $\boldsymbol{Z} = \boldsymbol{0}$. The same argument also holds for the dual case, $\boldsymbol{Z} = \|\boldsymbol{Z}\|\hat{\boldsymbol{b}}$ and $\boldsymbol{E} = \boldsymbol{0}$, hence for any linear combination of the two. The matrix $\boldsymbol{A}(t)$ is obtained from the projection operator, $\boldsymbol{T}_{BI}^T \left(\boldsymbol{I}_3 - \hat{\boldsymbol{b}}\hat{\boldsymbol{b}}^T\right) \boldsymbol{T}_{BI} = \left(\boldsymbol{I}_3 - \hat{\boldsymbol{b}}_I \hat{\boldsymbol{b}}_I^T\right)$. From the expression of $\hat{\boldsymbol{b}}_O$ in the orbit frame, $\hat{\boldsymbol{b}}_I$ is easily obtained in an inertially-fixed frame by means of the transformation $\hat{\boldsymbol{b}}_I = \left(\boldsymbol{T}_{IO}\boldsymbol{T}_{BO}^T\right) \hat{\boldsymbol{b}}_O$, where $\boldsymbol{T}_{BO}$ is given by Eq. (4). Without loss of generality, assume that the inertial frame is coincident

with $\mathbb{F}_O$ at time $t = t_0$, namely

$$\boldsymbol{T}_{IO} = \begin{pmatrix} \cos[n(t-t_o)] & 0 & \sin[n(t-t_o)] \\ 0 & 1 & 0 \\ -\sin[n(t-t_o)] & 0 & \cos[n(t-t_o)] \end{pmatrix}$$

Consider the case when the components of the Earth magnetic field are evaluated by means of a simple dipole model, such that the analytical derivation of $\ddot{\boldsymbol{A}}(t)$ is straightforward [11]. When $t = t^\star$, the error signal $\boldsymbol{e}^\star = k_\varepsilon \boldsymbol{E}(t^\star)$ is aligned with the local direction of $\hat{\boldsymbol{b}}^\star = \hat{\boldsymbol{b}}(t^\star)$, that is $\boldsymbol{e}^\star = ||\boldsymbol{e}||\hat{\boldsymbol{b}}^\star$. In this case, the expression of $J_{\ddot{\boldsymbol{A}}}$ is thus given by the quantity

$$J_{\ddot{\boldsymbol{A}}} = -\frac{2n^2 \sin^2(i)\left\{1 + 9\sin^2(i)\sin^4[n(t^\star - t_0)] - 6\sin^2(i)\sin^2[n(t^\star - t_0)]\right\}}{\left\{1 + 3\sin^2(i)\sin^2[n(t^\star - t_0)]\right\}^2}||\boldsymbol{e}^\star||^2 \tag{54}$$

which is a strictly negative periodic function of $t^\star$ with period $T/2$ for orbit inclination $i \neq 0$. Its maximum value can be evaluated at $t^\star = (1/2 + N)T/2 + t_0$ for $N = 0, 1, 2, \ldots$, such that

$$J_{\ddot{\boldsymbol{A}}} \leq -\frac{2n^2 \sin^2(i)}{1 + 3\sin^2(i)}||\boldsymbol{e}^\star||^2 \tag{55}$$

Repeating the argument for the dual case, $\boldsymbol{Z} = \|\boldsymbol{Z}\|\hat{\boldsymbol{b}}$ and $\boldsymbol{E} = \boldsymbol{0}$, and any other case in which the error signal $\boldsymbol{e}$ is parallel to the geomagnetic field $\boldsymbol{b}$, it is possible to state that

$$J_{\ddot{\boldsymbol{A}}} \leq -\frac{2k_{\min}^2 n^2 \sin^2(i)}{1 + 3\sin^2(i)}||\boldsymbol{Y}^\star||^2 = -\tilde{\mu}||\boldsymbol{Y}^\star||^2$$

where $k_{\min} = \min\{k_\varepsilon, k_\zeta\}$ and $\tilde{\mu} > 0$.

When $\boldsymbol{KY} \in \mathcal{N}_2$, that is, $k_\zeta \boldsymbol{Z} = \boldsymbol{u}$ and $k_\varepsilon \boldsymbol{E} = -\boldsymbol{u}$, the quadratic form $J_{\ddot{\boldsymbol{A}}} = (\boldsymbol{KY}^\star)^T \ddot{\boldsymbol{A}}(t^\star)(\boldsymbol{KY}^\star)$ vanishes, but it is possible to prove that the remaining term in the expression of $\dddot{V}(t^\star)$, namely $J_{\boldsymbol{B}} = -2(\boldsymbol{KB}^\star)^T \boldsymbol{A}(t^\star)(\boldsymbol{KB}^\star)$, is strictly negative, unless a very particular configuration is considered, unlikely to be encountered in practice and impossible to be maintained over time. From the definitions of $\boldsymbol{Z}$ and $\boldsymbol{E}$, the condition $\boldsymbol{KY} \in \mathcal{N}_2$ requires that all the vector quantities $\boldsymbol{Z}$, $\boldsymbol{E}$, $\boldsymbol{h}_d$, and $\boldsymbol{H}_d$ lie on the same plane, where $\boldsymbol{h}_d$ is parallel to the spacecraft pitch axis, whereas $\boldsymbol{H}_d$ is parallel to the normal to the orbit plane. From the definition of the vector $\boldsymbol{B}$ in Eq. (30), one can note that $J_{\boldsymbol{B}}$ vanishes if the second part of the vector $\boldsymbol{B}^\star = (\boldsymbol{0}^T, \boldsymbol{w}^T)^T$, namely $\boldsymbol{w} = \boldsymbol{T}_{BI}^T\left[\left(\boldsymbol{J}_a^{-1}\boldsymbol{T}_{BI}\boldsymbol{E}\right) \times \boldsymbol{h}_d\right]$ evaluated at $t = t^\star$, lies in the null space of the projection operator, that is, if $\boldsymbol{w}$ is parallel to $\boldsymbol{b}$. But this, in turn, requires that the pitch axis is perpendicular to the

geomagnetic field at time $t^\star$. All these conditions can be fulfilled if and only $\hat{\boldsymbol{b}}$ is perpendicular to both $\boldsymbol{h}_d$ and $\boldsymbol{H}_d$, that is, if the geomagnetic field is simultaneously perpendicular to the spacecraft pitch axis and the normal to the orbit plane, $\hat{\boldsymbol{o}}_2$. This is not possible if the component b_2 of the geomagnetic field along $\hat{\boldsymbol{o}}_2$ is different from zero and $\boldsymbol{E}$ and $\boldsymbol{Z}$ are collinear. It is thus possible to state that, when $b_2 \neq 0$, then $J_{\boldsymbol{B}} \leq -\bar{\mu}\|\boldsymbol{Y}^\star\|^2$, with $\bar{\mu} > 0$.

There is only one case, when b_2 vanishes, and this is the simple dipole model for an orbit inclination $i = 90$ deg. In this case an exponential convergence is no longer guaranteed at a theoretical level for the nominal system in Eq. (46). But the dipole model is oversimplified. The tilted dipole model accounts for a variation of the relative position of the geomagnetic field polar axis (which rotates with the Earth) with respect to the (inertially-fixed) orbit plane. Thus, in all practical cases and for a sufficiently detailed geomagnetic field model, the value of $J_{\boldsymbol{B}}$ remains negative and bounded as soon as b_2 becomes non-zero.

The determination of the bound $\bar{\mu}$ is rather cumbersome, and it depends on the values of the spacecraft moments of inertia, the magnitude of the desired angular momentum, and on the gains k_ζ and k_ε, and it is not reported here for the sake of conciseness. Nonetheless, the fact that a bound for the quadratic form $\boldsymbol{J}_{\boldsymbol{B}}$ exists in (almost) every operational condition implies that at least one of the two quadratic forms, $J_{\ddot{\boldsymbol{A}}}$ and $J_{\boldsymbol{B}}$, is different from zero when $\dot{V}$ vanishes. Thus $\dddot{V} \leq \dddot{V}_{\max} < 0$ allows for the determination of a finite bound of λ in Eq. (50), uniformly valid in t.

In fact, according to the considerations analyzed above, it is possible to write

$$\dddot{V}(t^\star, \boldsymbol{Y}^\star) \leq -\mu \, ||\boldsymbol{Y}^\star||^2 < 0$$

with $\mu = \min\{\tilde{\mu}, \bar{\mu}\}$. From Eq. (52), one gets that

$$V(t^\star + \delta) - V(t^\star) \leq -(\mu/6)||\boldsymbol{Y}^\star||^2\delta^3 + \mathcal{O}(\delta^4)$$

By taking into account the expression of the Lyapunov candidate function in Eq. (47), it is also

$$V(t^\star + \delta) - V(t^\star) \leq -\tilde{\lambda}(\delta)V(t^\star) + \mathcal{O}(\delta^4) \tag{56}$$

where $\tilde{\lambda}(\delta) = \mu\delta^3/(3k_{\max})$, with $k_{\max} = \max\{k_\varepsilon, k_\zeta\}$.

From the arguments reported above, it is possible to show that, for a sufficiently small δ, there

exists a $\lambda(\delta) > 0$ such that

$$V(t^\star + \delta) - V(t^\star) \leq -\lambda(\delta) V(t^\star) \tag{57}$$

Finally, by Eq. (51), the inequality in Eq. (50) is satisfied with the same $\lambda = \lambda(\delta)$ introduced in Eq. (57). Given the above considerations, the origin $\boldsymbol{Y} = \boldsymbol{0}$ is globally exponentially stable for the system in Eq. (46).

Consider now the case when $\bar{\gamma} \neq 0$. The hypotheses of Lemma 9.1 in Ref. [17] are satisfied. In particular, the origin $\boldsymbol{Y} = \boldsymbol{0}$ is a globally uniformly exponentially stable equilibrium point for the nominal system $\dot{\boldsymbol{Y}} = -\boldsymbol{A}(t)\boldsymbol{K}\,\boldsymbol{Y} - \boldsymbol{B}\,(t, \boldsymbol{Y})$ (see above), and the perturbation term satisfies the linear growth bound $\|\boldsymbol{g}(t, \boldsymbol{Y})\| = \|\boldsymbol{C}(t, \boldsymbol{Y})\| \leq \bar{\gamma}\, \|\boldsymbol{Y}\|$ for all $(t, \boldsymbol{Y}) \in [t_0,\ \infty) \times \mathbb{R}^6$, provided $\bar{\gamma} = |h_d|\, \delta_{\max}$, where $\delta_{\max} = \max\{|\delta_1|, |\delta_2|, |\delta_3|\}$. □

Note that the estimate of λ performed above on the basis of the simple dipole model is conservative. More complex models, such as the IGRF or the actual geomagnetic field, do not allow an analytical derivation of the bound, but they are characterized by a behavior in the time-domain with short-term oscillations that cause the value of V to decrease at a faster rate with respect to that determined from the simpler model.

References

[1] Avanzini, G., and Giulietti, F., "Magnetic Detumbling of a Rigid Spacecraft," *Journal of Guidance, Control, and Dynamics*, Vol. 35, No. 4, Jul.-Aug. 2012, pp. 1326-1334.
doi: 10.2514/1.53074

[2] Giulietti, F., Quarta, A.A., and Tortora, P., "Optimal Control Laws for Momentum-Wheel Desaturation Using Magnetorquers," *Journal of Guidance, Control, and Dynamics*, Vol. 29, No. 6, Nov.-Dec. 2006, pp. 1464-1468.
doi: 10.2514/1.23396

[3] Bruzzi, D., Tortora, P., Giulietti, F., and Galeone, P., "European Student Earth Orbiter: ESA's Educational Microsatellite Program," 27th Annual AIAA/USU Conference on Small Satellites, SSC13-IX-3, Logan, Utah, 10-15 Aug. 2013.

[4] Lovera, M., and Astolfi, A., "Spacecraft Attitude Control Using Magnetic Actuators," *Automatica*, Vol. 40, No. 8, Aug. 2004, pp. 1405-1414.
doi: 10.1016/j.automatica.2004.02.022

[5] Lovera, M., and Astolfi, A., "Global Magnetic Attitude Control of Inertially Pointing Spacecraft," *Journal of Guidance, Control, and Dynamics*, Vol. 28, No. 5, Sept.-Oct. 2005, pp. 1065-1067.
doi: 10.2514/1.11844

[6] Damaren, C.J., "Hybrid Magnetic Attitude Control Gain Selection," AIAA Guidance, Navigation, and Control Conference and Exhibit, AIAA 2007-6439, Hilton Head, South Carolina, 20-23 Aug. 2007.
doi: 10.2514/6.2007-6439

[7] Pulecchi, T., and Lovera, M., "Attitude Control of Spacecraft with Partially Magnetic Actuation," 17th IFAC Symposium on Automatic Control in Aerospace, Vol. 17, Part 1, ICT, Universitas Studii Tolosana, France, June 2007, pp. 609-614.
doi: 10.3182/20070625-5-FR-2916.00104

[8] Forbes, J.R., and Damaren, C.J., "Geometric Approach to Spacecraft Attitude Control Using Magnetic and Mechanical Actuation," *Journal of Guidance, Control, and Dynamics*, Vol. 33, No. 2, Mar.-Apr. 2010, pp. 590-595.
doi: 10.2514/1.46441

[9] Avanzini, G., de Angelis, E.L., and Giulietti, F., "Spin-Axis Pointing of a Magnetically Actuated Spacecraft," *Acta Astronautica*, Vol 94, Issue 1, Jan.-Feb. 2014, pp. 493-501.
doi: 10.1016/j.actaastro.2012.10.035

[10] Trégouët, J.F., Arzelier, D., Peaucelle, D., Pittet, C., and Zaccarian, L., "Reaction Wheels Desaturation Using Magnetorquers and Static Input Allocation," *IEEE Transactions on Control Systems Technology*, Vol. 23, No. 2. Mar. 2015.
doi: 10.1109/TCST.2014.2326037

[11] Wertz, J.R., *Spacecraft Attitude Determination and Control*, Kluwer, Dordrecht, The Netherlands, 1978, Chs. 5 and 17.

[12] *International Geomagnetic Reference Field*, http://www.ngdc.noaa.gov/IAGA/vmod/igrf.html [retrieved on August 1st, 2014].

[13] Wie, B., *Space Vehicle Dynamics and Control*, American Institute of Aeronautics and Astronautics, Inc., Reston, VA, 1998, Ch. 7.

[14] Stickler, A.C., and Alfriend, K., "Elementary Magnetic Attitude Control System," *Journal of Spacecraft and Rockets*, Vol. 13, No. 5, Sept.-Oct. 1976, pp. 282-287.
doi: 10.2514/3.57089

[15] Avanzini, G., de Angelis, E.L., and Giulietti, F., "Acquisition of a Desired Pure Spin Condition for a Magnetically Actuated Spacecraft," *Journal of Guidance, Control, and Dynamics*, Vol. 36, No. 6,

Nov.-Dec. 2013, pp. 1816-1821.

doi: 10.2514/1.59364

[16] Beletskii, V.V., *Motion of an Artificial Satellite about its Center of Mass*, (Transl. from Russian), Israel Program for Scientific Translations, Jerusalem, Israel, 1966, pp. 13-19.

[17] Khalil, H.K., *Nonlinear Systems*, Third Edition, Prentice-Hall, Upper Saddle River, NJ, 2001, Chs. 8 and 9.

[18] Bronshtein, I.N., Semendyayev, K.A., Musiol, G., and Muehlig, H., *Handbook of Mathematics*, Fifth Edition, Springer-Verlag, New York, 2007, Ch. 6.